Research Square

Preprints are preliminary reports that have not undergone peer review.
They should not be considered conclusive, used to inform clinical practice,
or referenced by the media as validated information.

Fine mapping and candidate gene identification of QBp.caas-6A for black point resistance in wheat

Panpan Wang
Chinese Academy of Agricultural Sciences
Yue Zhang
Chinese Academy of Agricultural Sciences
Mengjuan Gao
Chinese Academy of Agricultural Sciences
Qiang Li
Chinese Academy of Agricultural Sciences
Shengnan Zhai
Shandong Academy of Agricultural Sciences
Baomin Zhang
Henan Join Hope Xinke Seed Co., Ltd.
Xianchun Xia
Chinese Academy of Agricultural Sciences
Yan Zhang
Chinese Academy of Agricultural Sciences
Xiaoting Xu
xuxiaoting@caas.cn

Chinese Academy of Agricultural Sciences
Jindong Liu
Chinese Academy of Agricultural Sciences

Research Article

Keywords: wheat, black point resistance, fine mapping, candidate gene, molecular marker

Posted Date: November 24th, 2026

DOI: https://doi.org/10.21203/rs.3.rs-11626287/v1

License: This work is licensed under a Creative Commons Attribution 4.0 International License.
Read Full License

Additional Declarations: No competing interests reported.

Abstract

Black point (BP), characterized by discoloration around the embryo of wheat grains, reduces grain quality and commodity grade. The stable quantitative trait locus (QTL) *QBp.caas-6A* for BP resistance was previously detected across five environments in a recombinant inbred line (RIL) population derived from Linmai 2 and Zhong 892. In the present study, nine heterozygous recombinants were identified from a secondary mapping population using 12 kompetitive allele-specific PCR (KASP) markers. Evaluation of progeny from these recombinants delimited *QBp.caas-6A*to a 1.8-Mb interval (77.5–79.3 Mb) on IWGSC RefSeq v1.1 that contains 13 high-confidence genes. Combined analysis of parental sequence variation and gene expression identified *TraesCS6A02G109000* and *TraesCS6A02G110000*as candidate genes for *QBp.caas-6A*. The KASP marker *K79* was evaluated in a diversity panel of 125 wheat cultivars and was associated with reduced BP incidence in four of five environments. Metabolomic profiling showed the greatest divergence between the resistant and susceptible near-isogenic lines at 15 days after anthesis, with several lipids showing the largest difference in abundance. These results provide a basis for map-based cloning of *QBp.caas-6A*, a linked marker for marker-assisted selection of the locus, and further investigation of metabolic processes associated with BP resistance.

Key message

***QBp.caas-6A* was delimited to a 1.8-Mb interval containing 13 genes, and *TraesCS6A02G109000* and *TraesCS6A02G110000* were prioritized as candidates.**

Introduction

Black point (BP) is a widespread grain-discoloration problem of bread wheat (*Triticum aestivum* L.) and is characterized by dark-brown to black pigmentation around the embryo, sometimes extending along the ventral surface of the kernel (Conner and Kuzyk 1988). Because affected grain is visually unacceptable, BP lowers commodity grade and market value and can lead to rejection of grain lots when tolerance thresholds are exceeded (Lehmensiek et al. 2004; Liu et al. 2016). BP has also been associated with changes in test weight, falling number, flour yield, and dough properties, although the magnitude of these effects varies among studies and levels of infection (Fernandez et al. 2011). Severely affected seeds may show reduced germination, emergence, and early seedling growth (Fernandez et al. 2014; Li et al. 2020). Moreover, some fungi recovered from discolored kernels can produce fumonisins or *Alternaria* toxins, creating a potential food- and feed-safety concern, although the presence of BP symptoms alone does not establish mycotoxin contamination (Busman et al. 2012; Desjardins et al. 2007; Masiello et al. 2020).

The origin of BP symptoms is complex because pathogen infection, environmental conditions, and host biochemical responses can all contribute to their development. Several fungi, particularly *Alternaria alternata*, *Bipolaris sorokiniana* and *Fusarium proliferatum*, have been associated with BP (Al-Sadi 2021; Busman et al. 2012; Kumar et al. 2002; Somma et al. 2019), but fungi may also be isolated from

symptomless kernels, and a direct relationship between fungal colonization and discoloration has not always been demonstrated (Lehmensiek et al. 2004). High humidity, rainfall, and temperature stress during grain filling and ripening strongly favor symptom development. These biotic and abiotic stresses are thought to disturb redox homeostasis and promote oxidation of phenolic substrates by peroxidase and polyphenol oxidase, followed by the formation of quinones and dark pigments (Fernandez et al. 2011; Mak et al. 2006). Although agronomic, chemical, and biological measures may reduce disease development, breeding resistant cultivars remains a practical and economical foundation for BP management.

Linkage mapping and genome-wide association studies have identified resistance loci on several wheat chromosomes, confirming the availability of useful genetic variation but also revealing a dispersed and complex genetic architecture (Liu et al. 2016, 2017). Relatively few genetic studies of BP have been conducted and many reported loci explain small-to-moderate proportions of the phenotypic variation, have been detected in only a subset of environments, or remain defined by broad marker intervals (Chen et al. 2025; Lehmensiek et al. 2004; Liu et al. 2016, 2017; Lv et al. 2020). No BP resistance gene has yet been cloned. This limitation constrains both causal analysis of host response and the development of markers that reliably track resistance alleles in breeding populations.

QBp.caas-6A is a particularly relevant locus for addressing this gap. It was initially identified between 73.7 and 115.0 Mb using a recombinant inbred line (RIL) population derived from Linmai 2 and Zhong 892, and was detected in five of seven environments, explaining 3.7–8.7% of the phenotypic variation (Liu et al. 2016). In this study, we fine-mapped *QBp.caas-6A* to a 1.8-Mb interval, prioritized *TraesCS6A02G109000* and *TraesCS6A02G110000* through parental resequencing and transcriptome analysis, evaluated the linked KASP marker *K79* in a diversity panel of 125 wheat cultivars, and characterized metabolic differences between contrasting near-isogenic lines. These results provide a foundation for further identifying the causal gene and evaluating *QBp.caas-6A* in wheat breeding materials.

Materials and methods

Plant materials

Because no residual heterozygous lines were found in the original Linmai 2/Zhong 892 mapping population, two recombinant inbred lines (RILs), RIL4546 and RIL4621, were crossed to develop a secondary mapping population. RIL4546 carries three black point resistance QTLs (*QBp.caas-2AL*, *QBp.caas-6A*, and *QBp.caas-7AL.1*), whereas RIL4621 only carries *QBp.caas-2AL* and *QBp.caas-7AL.1*. These two RILs are highly similar in genetic background and flowering time, differing primarily at the *QBp.caas-6A* locus. To develop the near-isogenic lines (NILs), the F_1 plants from the RIL4546 × RIL4621 cross were self-pollinated to generate an F_2 population. Heterozygous recombinant plants at *QBp.caas-6A* were identified via genotyping and advanced through greenhouse generation ($F_{2:4}$) and subsequent field selections (F_5 and F_6 generation in Xinxiang, autumn-sown). Homozygous lines carrying contrasting

allels at *QBp.caas-6A* were selected from these advanced generations using marker-assisted selection, generating a pair of near-isogenic lines (NILs) designated as NIL-R (Zhong 892 allele) and NIL-S (Linmai 2 allele).

Field trials and BP evaluation

Approximately 280 progeny from each heterozygous recombinant were sown in 3-m rows, with 31 seeds per row, 10 cm between plants and 25 cm row spacing at Xinxiang, Henan province, during the 2021–2022, 2022–2023, and 2023–2024 cropping seasons. The NILs were also planted at Xinxiang (35.30°N, 113.90°E), Henan province, with around 50 seeds per 1-m row and 25 cm spacing during the 2022–2023 and 2023–2024 cropping seasons. The diversity panel of 125 cultivars was evaluated in randomized complete blocks with three replicates at Anyang (36.10°N, 114.38°E), Henan Province, during the 2012–2013, 2013–2014 and 2014–2015 cropping seasons, and at Suixi (33.92°N, 114.77°E), Anhui Province, during the 2012–2013 and 2013–2014 cropping seasons. Approximately 50 seeds of each cultivar were planted in 1-m rows with 20 cm spacing. All field trials were managed according to local agronomic practices.

BP evaluation was conducted on mature grains after a post-harvest period of at least 15 days. BP incidence was quantified by examining 200 kernels per line or individual plant and recording the proportion displaying characteristic embryo discoloration. All assessments were performed by the same trained evaluator under standardized illumination conditions to maintain scoring consistency.

Whole-genome resequencing of Zhong 892 and Linmai 2

Whole-genome resequencing of Zhong 892 and Linmai 2 was performed by Novogene (Beijing, China). Genomic DNA isolated from young leaves using CTAB extraction was assessed spectrophotometrically before library preparation. DNA was randomly sheared into 200–500 bp fragments and processed into sequencing libraries by adapter ligation. Library quality was assessed using Bioanalyzer and Qubit systems before sequencing on an Illumina HiSeq platform. After low-quality reads were removed, the clean reads were aligned to IWGSC RefSeq v1.1 (The International Wheat Genome Sequencing Consortium et al. 2018) using BWA (Li and Durbin 2009). Variants were called using SAMtools (Li et al. 2009) and GATK (McKenna et al. 2010), and high-confidence SNPs and InDels were functionally annotated using ANNOVAR (Wang et al. 2010).

Development of molecular markers

SNPs within the mapping region were identified from the whole-genome resequencing data of Linmai 2 and Zhong 892. For each SNP, 70 bp on either side was submitted to PolyMarker (http://www.polymarker.info/) for KASP assay design (Ramirez-Gonzalez et al. 2015), and chromosome-specific primers were prioritized. Each KASP assay contained two allele-specific forward primers with

FAM or HEX fluorescent tails, 5'-GAAGGTGACCAAGTTCATGCT-3' and 5'-GAAGGTCGGAGTCAACGGATT-3', respectively, and a common reverse primer. Each PCR reaction contained 2.0 µL DNA template at ~ 50 ng/µL, 2.0 µL KASP 2× Master Mix and 0.0336 µL KASP primer mix containing each forward primer at 12 µM and the common reverse primer at 30 µM. PCR was performed at 94°C for 15 min, followed by 10 touch-down PCR cycles at 94°C for 20 s and 65°C for 60 s with a decrease of 0.8°C per cycle, and then 35 cycles at 94°C for 20 s and 57°C for 60 s using a Hydrocycler (LGC, Hoddesdon, UK). Fluorescence was read using a PHEstar microplate reader (BMG Labtech, Ortenberg, Germany) and genotypes were called using KlusterCaller™ v2.24.0.11 (LGC, Hoddesdon, UK).

Transcriptome analysis and quantitative reverse-transcription PCR (qRT-PCR)

Developing grains from the middle of the spikes of NIL-R and NIL-S were collected at 15 days after anthesis (DAA) for RNA sequencing, with three biological replicates per NIL, and sent to Novogene for library preparation and sequencing. Total RNA was extracted using TRIzol, and RNA purity and integrity were assessed using a NanoDrop spectrophotometer, agarose gel electrophoresis, and an Agilent 2100 Bioanalyzer to ensure RNA integrity number ≥ 8.0. Libraries were prepared by RNA fragmentation and cDNA synthesis and sequenced as 150-bp paired-end reads on an Illumina HiSeq 4000 platform. After quality filtering, clean reads were aligned to the IWGSC RefSeq v1.1 using HISAT2 (Kim et al. 2019). Gene expression was estimated as fragments per kilobase of transcript per million mapped fragments (FPKM). Differentially expressed genes were identified using DESeq2 (Love et al. 2014), with adjusted *P*-value < 0.05 and |log2 fold change (FC)| > 0.5 as thresholds.

For qRT-PCR, RNA was extracted using an RNAprep Pure Plant Kit following the manufacturer's instructions (Cat. No. DP441, Tiangen, Beijing) and reverse-transcribed using a PrimeScript RT Reagent Kit (Cat. No. RR036B, Takara, Japan). qRT-PCR was performed in a Bio-Rad CFX system (https://www.bio-rad.com/) using 2 × Universal SYBR Green Fast qPCR Mix (Cat. No. RK21203, ABclonal, Wuhan) and three biological replicates per sample. The wheat *Actin* gene was used as the internal control. Relative expression was calculated using the $2^{-\Delta\Delta CT}$ method (Livak and Schmittgen 2001).

Metabolic analysis of NILs

Developing grains of NIL-R and NIL-S were collected at 5, 10, 15 and 20 DAA at Xinxiang, Henan Province, in 2022 with five biological replicates per sample per stage and stored at − 80°C. For metabolite extraction, 100 mg of tissue was pulverized in liquid nitrogen and homogenized in pre-chilled 80% methanol through vigorous vortexing. Following a 5-min incubation on ice, samples were centrifuged at 15,000 × g for 20 min at 4°C. The supernatant was diluted with LC-MS grade water to a final methanol concentration of 53% and centrifuged again under the same conditions. The clarified extracts were analyzed by UPLC–MS/MS as described by Want et al. (2013). Metabolites were annotated against the KEGG pathway database (https://www.genome.jp/kegg/pathway.html). Principal component analysis

(PCA) and partial least-squares discriminant analysis were performed using the metaX platform (Wen et al. 2017). Differentially accumulated metabolites were identified using variable importance in projection scores (VIP) > 1.0, Student's *t*-test $P < 0.05$, and FC ≥ 1.20 or ≤ 0.83.

Results

Analysis of resequencing data from Zhong 892 and Linmai 2

Whole-genome comparison with IWGSC RefSeq v1.1 identified 22,593,207 SNPs in Zhong 892, including 67,983 non-synonymous, 293 stop-gain, and 1,033 stop-loss variants. In Linmai 2, 23,104,419 SNPs were identified, including 63,002 non-synonymous, 957 stop-gain, and 315 stop-loss variants. SNPs within the original *QBp.caas-6A* mapping interval at 73.7–115.0 Mb were selected for conversion to KASP markers.

Fine mapping of QBp.caas-6A

A total of 12 KASP markers were developed within or flanking the initial mapping region (Table S1). Screening 324 $F_{2:4}$ lines and 1,940 $F_{4:5}$ lines identified seven (L1–L7) and two (L8, L9) heterozygous recombinant lines, respectively. BP incidence was compared between homozygous progeny carrying the contrasting genotypes at *QBp.caas-6A*. Significant differences were detected between genotypes derived from L2, L3, L5, L8 and L9 ($P < 0.05$), while no significant differences were detected for L1, L4, L6 or L7 (Fig. 1; Table S2). The result delimited *QBp.caas-6A* to a 1.8-Mb interval between KASP markers *K77* (77.5 Mb) and *K79* (79.3 Mb) according to IWGSC RefSeq v1.1.

Analysis of candidate genes of QBp.caas-6A

The *QBp.caas-6A* interval contained 13 high-confidence genes according to IWGSC RefSeq v1.1 annotation (Table S3). Collinearity analysis showed that gene order within the interval was conserved between Chinese Spring and the other wheat genomes examined (Fig. S1). RNA-seq analysis showed that only *TraesCS6A02G109000* and *TraesCS6A02G110000* were differentially expressed between NIL-R and NIL-S within the interval at 15 DAA (Fig. 2a; Table S4). *TraesCS6A02G109000* was predicted to encode an activator of heat shock protein 90 ATPase (Aha1), whereas *TraesCS6A02G110000* was predicted to encode a glucan endo-1,3-β-glucosidase belonging to the glycoside hydrolase superfamily. qRT-PCR confirmed the differential expression of both genes (Fig. 2b; Table S5). *TraesCS6A02G109000* was expressed at a higher level in NIL-R than in NIL-S, whereas *TraesCS6A02G110000* was expressed at a higher level in NIL-S. Missense mutations between the parents were identified in both genes (Table 1); thus, *TraesCS6A02G109000* and *TraesCS6A02G110000* were prioritized as candidate genes for *QBp.caas-6A*.

Table 1
Predicted candidate genes of *QBp.caas-6A*

Gene ID [a]	Nucleotide (amino acid) change [b]	Gene annotation
TraesCS6A02G109000	GGTTAGTTGTTTAAACTACACATG > GG	Activator of 90 kDa heat shock protein ATPase
TraesCS6A02G110000	Exon1: C50T (A17V), T77C (L26S)	Glucan endo-1,3-beta-glucosidase

[a] Gene ID and annotation information were retrieved from the Chinese Spring reference genome (https://urgi.versailles.inra.fr/blast_iwgsc/)

[b] Numbers represent the positions of polymorphic sites in the open reading frame of candidate genes between Linmai 2 and Zhong 892; the location of the start codon was set as 1

Genetic effect analysis of QBp.caas-6A

The KASP marker *K79*, located at 79,268,741 bp and targeting a T486C variant predicted to cause a V162A substitution in *TraesCS6A02G110100*, was used to genotype the diversity panel of 125 wheat cultivars. The genotype frequencies were 43.2% Zhong 892 allele (TT), 39.2% Linmai 2 allele (CC) and 17.6% heterozygotes (Table S6). Within-environment *t*-tests showed that cultivars carrying the Zhong 892 allele had significantly lower BP incidence than those carrying the Linmai 2 allele (CC) in all five environments except AY2014 (Fig. 3a, b).

Metabolites associated with BP resistance

To characterize metabolic variation associated with BP resistance, developing grains of NIL-R and NIL-S were analyzed by untargeted UPLC–MS/MS at 5, 10, 15, and 20 DAA. Of 1,528 detected metabolites, lipids and lipid-like molecules constituted the largest class (30.37%), followed by organic acids and derivatives (15.32%), phenylpropanoids and polyketides (13.29%), organoheterocyclic compounds (12.59%), and organic oxygen compounds (9.24%), together accounting for over 80% of the metabolome (Fig. S2). PCA showed that development stage was the dominant source of variance (PC1 39.48%, PC2 10.47%; 49.95% cumulative), with clear stage separation and genotype separation within stages, most pronounced at 15 DAA (Fig. 4a). Pairwise comparisons identified 69, 47, 143, and 110 differentially accumulated metabolites at 5, 10, 15, and 20 DAA, respectively (Table S7; Fig. 4b); of these, 26, 23, 37, and 39 were higher abundance, whereas 43, 24, 106, and 71 were lower abundance in the NIL-S at each stage. The greater number of metabolites with lower abundance in NIL-S at 15 and 20 DAA indicates that NIL-R sustains higher levels of a broad set of metabolites during mid–late grain filling.

Although no single metabolite was consistently differentially accumulated across all four stages (Fig. S3a), several putatively annotated lipids exhibited highly significant changes within individual stages (Fig. S3b). At 5 DAA, docosahexaenoic acid had a 55.6-fold lower abundance in NIL-S than in NIL-R. Conversely, at 15 DAA, phosphatidylethanolamine (PE 18:1_18:2) and monogalactosyldiacylglycerol (MGDG 16:0_18:2) showed the largest increases in NIL-S, with FC of 31.8 and 23.3, respectively. These

contrasting patterns indicate stage-dependent differences in lipid metabolism rather than a uniform increase or decrease in lipid abundance in either NIL (Table S7). Overall, the contrasting *QBp.caas-6A* genotypes were associated with extensive developmental differences in the grain metabolome, with the greatest divergence at 15 DAA and prominent changes in lipid-associated metabolism and membrane-related signaling.

Discussion

Comparison of QBp.caas-6A with previously reported loci

Black point is a widespread grain-quality problem in wheat-growing regions worldwide (Conner and Kuzyk 1988; Cromey and Mulholland 1988; Lehmensiek et al. 2004; Liu et al. 2016; Sissons et al. 2010). In the present study, QBp.*caas-6A* was delimited to a 1.8-Mb physical interval between 77.5 and 79.3 Mb on IWGSC RefSeq v1.1 (Fig. 1). This interval is physically distinct from previously identified BP-associated loci on chromosome 6A, including the locus associated with *AX_108821301* at around 94.2 Mb (Liu et al. 2017), q.*bp_7* between *AX-108877487* and *AX111651180* at 3.2 and 6.4 Mb, respectively (Tang et al. 2022), and two loci associated with *Excalibur_c10055_221* at 28.0 Mb, and with *GENE-4167_145* and *BS00099401_51* at 611.3 and 613.3 Mb, respectively (Lv et al. 2020). The refined position of *QBp.caas-6A* provides a basis for map-based cloning and for developing markers suitable for molecular breeding applications of this locus.

Candidate genes underlying QBp.caas-6A

Thirteen high-confidence genes were in the refined interval of *QBp.caas-6A* (Table S3). Analysis of parental sequence variation and NIL expression profiles prioritized *TraesCS6A02G109000* and *TraesCS6A02G110000* as candidate genes (Fig. 3; Table S3). *TraesCS6A02G109000* is predicted to encode an activator of HSP90 ATPase (Aha1), suggesting a potential role in regulating HSP90-dependent protein homeostasis. HSP90 co-chaperones RAR1 and SGT1 to support plant immune receptor function (Chen et al. 2010; Kadota et al. 2008; Takahashi et al. 2003). BP development is associated with oxidative stress and host enzymatic browning: excessive reactive oxygen species can promote oxidation of phenolic compounds and formation of dark pigments (Li et al. 2020). An Aha1 allele that alters the HSP90 cycle could therefore affect the stability of stress- or defense-signaling proteins, indirectly improving control of pathogen growth, oxidative injury or both. However, the expression difference alone does not establish a direct impact on HSP90 ATPase activity or downstream pathogen restriction. Functional validation, including the assessment of its interaction with HSP90/SGT1 complexes and its necessity for ROS homeostasis during infection, is required to elucidate its contribution to BP resistance.

TraesCS6A02G110000 is predicted to encode a glucan endo-1,3-β-glucosidase. β-1,3-Glucanases play key roles in plant development, transport through plasmodesmata, abiotic-stress responses, and defense against fungal pathogens (Balasubramanian et al. 2012). In maize, a β-1,3-glucanase gene was induced by biotic and abiotic stresses and by growth hormones (Xie et al. 2015). In wheat, early β-1,3-

glucanase accumulation and recognition of fungal β-glucans have been associated with resistance to *Septoria tritici* (Shetty et al. 2009), and transgenic expression of a β-1,3-glucanase enhanced resistance to Fusarium head blight (Mackintosh et al. 2007). In this study, Tra*esCS6A02G110000* was expressed significantly higher in NIL-S, which is inconsistent with a simple model in which greater transcript abundance confers resistance. However, two SNPs in this gene, C50T and T77C, causing A17V and L26S substitutions, respectively, warrant further investigation. Transgenic complementation and CRISPR-Cas9-mediated gene editing will be required to determine whether either candidate is the causal gene at *QBp.caas-6A*.

Evaluation of linked KASP marker K79

Although *K79* targets a nonsynonymous variant in *TraesCS6A02G110100*, rather than either prioritized candidate gene, it was associated with lower BP incidence in cultivars carrying the Zhong 892 allele in four of five environments examined (Fig. 3), indicating potential utility for marker-assisted selection of *QBp.caas-6A*. Its transferability to other breeding populations requires further validation.

Metabolites related to BP resistance

Metabolite profiles varied across stages (Fig. S3). Lipids and lipid-like molecules constituted the largest class in the detected metabolome, and several putatively annotated lipids were among the most strongly altered metabolites. Lipids are structural components of cellular membranes and can participate in plant defense signaling, as signaling mediators, precursors of bioactive molecules and regulators of reactive oxygen species formation (Kuźniak and Gajewska 2024; Lim et al. 2017; Mamode Cassim et al. 2019). Soluble inositol phosphates act as cofactors in immune signaling medidated by tomato NRC2 (Ma et al. 2024). In addition, negatively charged phospholipids support the plasma-membrane localization and cell death activity of certain NLR proteins (Saile et al. 2021). In the present study, the clearest separation and the largest number of differentially accumulated metabolites between the NILs were observed at 15 DAA (Fig. 4a, b). The concurrent differences in candidate-gene expression and the higher abundance of PE and MGDG in the NIL-S at this stage suggest a possible association between the *QBp.caas-6A* interval and membrane-lipid profiles. However, these observations do not establish direct regulation of these metabolites by either candidate gene. Identification and functional validation of the causal gene, together with targeted lipid analysis, are needed to test the proposed relationship.

Conclusion

QBp.caas-6A was delimited to a 1.8-Mb interval at 77.5–79.3 Mb, which is physically distinct from previously reported black point resistance loci on chromosome 6A. Analysis of parental sequence variation and gene expression prioritized *TraesCS6A02G109000* and *TraesCS6A02G110000* as candidate genes. The linked KASP marker *K79* was evaluated in a diversity panel of 125 wheat cultivars. Further functional validation by transgenic complementation and CRISPR-Cas9-mediated gene editing is needed to identify the causal gene.

Declarations

Conflicts of interest statement

The authors declare that they have no conflict of interest.

Author Contribution

P.W.–data analysis, manuscript writing and revision; Yan Z.–population development, phenotyping and manuscript drafting; M.G., Q.L., S.Z. and B.Z.–sample collection and manuscript revision; Xianchun X. and Yan Z.–funding acquisition and manuscript review; Xiaoting X.–data analysis and manuscript review; J.L.–funding acquisition, project conception, manuscript writing and review.

Acknowledgements

This work was supported by the National Natural Science Foundation of China (32272186), Beijing Natural Science Foundation (6242031), Central Public-interest Scientific Institution Basal Research Fund (No. S2026QZ20), the CAAS Science and Technology Innovation Program, Shenzhen Key Science and Technology Program (KCXFZ20240903092403005), Henan Provincial Joint Research Project on Agricultural Elite Varieties (2026–2030) (2026010104) and Shandong Provincial Natural Science Foundation Projects (ZR2023MC205 and ZR2023MC155).

Data Availability

All data supporting the findings of this study are available within the paper and its Supplementary Information. Any additional data that support the findings of this study are available from the corresponding authors upon reasonable request.

References

1. Al-Sadi AM (2021) Bipolaris sorokiniana-induced black point, common root rot, and spot blotch diseases of wheat: A review. Front Cell Infect Microbiol 11:584899. https://doi.org/10.3389/fcimb.2021.584899
2. Balasubramanian V, Vashisht D, Cletus J, Sakthivel N (2012) Plant β-1,3-glucanases: their biological functions and transgenic expression against phytopathogenic fungi. Biotechnol Lett 34:1983–1990. https://doi.org/10.1007/s10529-012-1012-6
3. Busman M, Desjardins AE, Proctor RH (2012) Analysis of fumonisin contamination and the presence of Fusarium in wheat with kernel black point disease in the United States. Food Addit Contaminants: Part A 29:1092–1100. https://doi.org/10.1080/19440049.2012.671787

4. Chen L, Hamada S, Fujiwara M, Zhu T, Thao NP, Wong HL, Krishna P, Ueda T, Kaku H, Shibuya N, Kawasaki T, Shimamoto K (2010) The Hop/Sti1-Hsp90 chaperone complex facilitates the maturation and transport of a PAMP receptor in rice innate immunity. Cell Host Microbe 7:185–196. https://doi.org/10.1016/j.chom.2010.02.008
5. Chen T, Li L, Liu D, Tian Y, Li L, Zeng J, Rasheed A, Cao S, Xia X, He Z, Liu J, Zhang Y (2025) Genome wide linkage mapping for black point resistance in a recombinant inbred line population of Zhongmai 578 and Jimai 22. J Integr Agric 24:3311–3321. https://doi.org/10.1016/j.jia.2023.12.039
6. Conner RL, Kuzyk AD (1988) Effectiveness of fungicides in controlling stripe rust, leaf rust, and black point in soft white spring wheat. Can J Plant Pathol 10:321–326. https://doi.org/10.1080/07060668809501706
7. Cromey MG, Mulholland RI (1988) Blackpoint of wheat: Fungal associations, cultivar susceptibility, and effects on grain weight and germination. New Z J Agricultural Res 31:51–56. https://doi.org/10.1080/00288233.1988.10421363
8. Desjardins AE, Busman M, Proctor RH, Stessman R (2007) Wheat kernel black point and fumonisin contamination by Fusarium proliferatum. Food Addit Contam 24:1131–1137. https://doi.org/10.1080/02652030701513834
9. Fernandez MR, Sissons M, Conner RL, Wang H, Clarke JM (2011) Influence of biotic and abiotic factors on dark discoloration of durum wheat kernels. Crop Sci 51:1205–1214. https://doi.org/10.2135/cropsci2010.07.0433
10. Fernandez MR, Wang H, Singh AK (2014) Impact of seed discolouration on emergence and early plant growth of durum wheat at different soil gravimetric water contents. Can J Plant Pathol 36:509–516. https://doi.org/10.1080/07060661.2014.957242
11. Kadota Y, Amigues B, Ducassou L, Madaoui H, Ochsenbein F, Guerois R, Shirasu K (2008) Structural and functional analysis of SGT1-HSP90 core complex required for innate immunity in plants. EMBO Rep 9:1209–1215. https://doi.org/10.1038/embor.2008.185
12. Kim D, Paggi JM, Park C, Bennett C, Salzberg SL (2019) Graph-based genome alignment and genotyping with HISAT2 and HISAT-genotype. Nat Biotechnol 37:907–915. https://doi.org/10.1038/s41587-019-0201-4
13. Kumar J, Schafer P, Huckelhoven R, Langen G, Baltruschat H, Stein E, Nagarajan S, Kogel KH (2002) Bipolaris sorokiniana, a cereal pathogen of global concern: cytological and molecular approaches towards better control. Mol Plant Pathol 3:185–195. https://doi.org/10.1046/j.1364-3703.2002.00120.x
14. Kuźniak E, Gajewska E (2024) Lipids and lipid-mediated signaling in plant-pathogen interactions. Int J Mol Sci 25:7255. https://doi.org/10.3390/ijms25137255
15. Lehmensiek A, Campbell AW, Sutherland MW, Williamson PM, Michalowitz M, Daggard GE (2004) QTLs for black-point resistance in wheat and the identification of potential markers for use in breeding programmes. Plant Breeding 123:410–416. https://doi.org/10.1111/j.1439-0523.2004.01013.x

16. Li H, Durbin R (2009) Fast and accurate short read alignment with Burrows-Wheeler transform. Bioinformatics 25:1754–1760. https://doi.org/10.1093/bioinformatics/btp324
17. Li H, Handsaker B, Wysoker A, Fennell T, Ruan J, Homer N, Marth G, Abecasis G, Durbin R, Subgroup GPDP (2009) The sequence alignment/map format and SAMtools. Bioinformatics 25:2078–2079. https://doi.org/10.1093/bioinformatics/btp352
18. Li Q, Xu K, Wang S, Li M, Jiang Y, Liang X, Niu J, Wang C (2020) Enzymatic browning in wheat kernels produces symptom of black point caused by Bipolaris sorokiniana. Front Microbiol 11:526266. https://doi.org/10.3389/fmicb.2020.526266
19. Lim GH, Singhal R, Kachroo A, Kachroo P (2017) Fatty acid- and lipid-mediated signaling in plant defense. Annu Rev Phytopathol 55:505–536. https://doi.org/10.1146/annurev-phyto-080516-035406
20. Liu J, He Z, Rasheed A, Wen W, Yan J, Zhang P, Wan Y, Zhang Y, Xie C, Xia X (2017) Genome-wide association mapping of black point reaction in common wheat (*Triticum aestivum* L). BMC Plant Biol 17:220. https://doi.org/10.1186/s12870-017-1167-3
21. Liu J, He Z, Wu L, Bai B, Wen W, Xie C, Xia X (2016) Genome-wide linkage mapping of QTL for black point reaction in bread wheat (*Triticum aestivum* L). Theor Appl Genet 129:2179–2190. https://doi.org/10.1007/s00122-016-2766-3
22. Livak KJ, Schmittgen TD (2001) Analysis of relative gene expression data using real-time quantitative PCR and the $2^{-\Delta\Delta CT}$ method. Methods 25:402–408. https://doi.org/10.1006/meth.2001.1262
23. Love MI, Huber W, Anders S (2014) Moderated estimation of fold change and dispersion for RNA-seq data with DESeq2. Genome Biol 15:550. https://doi.org/10.1186/s13059-014-0550-8
24. Lv G, Dong Z, Wang Y, Geng J, Li J, Lv X, Sun C, Ren Y, Zhang J, Chen F (2020) Identification of genetic loci of black point in Chinese common wheat by genome-wide association study and linkage mapping. Plant Dis 104:2005–2013. https://doi.org/10.1094/pdis-12-19-2733-re
25. Ma S, An C, Lawson AW, Cao Y, Sun Y, Tan EYJ, Pan J, Jirschitzka J, Kummel F, Mukhi N, Han Z, Feng S, Wu B, Schulze-Lefert P, Chai J (2024) Oligomerization-mediated autoinhibition and cofactor binding of a plant NLR. Nature 632:869–876. https://doi.org/10.1038/s41586-024-07668-7
26. Mackintosh CA, Lewis J, Radmer LE, Shin S, Heinen SJ, Smith LA, Wyckoff MN, Dill-Macky R, Evans CK, Kravchenko S, Baldridge GD, Zeyen RJ, Muehlbauer GJ (2007) Overexpression of defense response genes in transgenic wheat enhances resistance to Fusarium head blight. Plant Cell Rep 26:479–488. https://doi.org/10.1007/s00299-006-0265-8
27. Mak Y, Willows RD, Roberts TH, Wrigley CW, Sharp PJ, Copeland L (2006) Black point is associated with reduced levels of stress, disease- and defence-related proteins in wheat grain. Mol Plant Pathol 7:177–189. https://doi.org/10.1111/j.1364-3703.2006.00330.x
28. Mamode Cassim A, Gouguet P, Gronnier J, Laurent N, Germain V, Grison M, Boutté Y, Gerbeau-Pissot P, Simon-Plas F, Mongrand S (2019) Plant lipids: Key players of plasma membrane organization and function. Prog Lipid Res 73:1–27. https://doi.org/10.1016/j.plipres.2018.11.002

29. Masiello M, Somma S, Susca A, Ghionna V, Logrieco A, Franzoni M, Ravaglia S, Meca G, Moretti A (2020) Molecular identification and mycotoxin production by Alternaria species occurring on durum wheat, showing black point symptoms. Toxins 12:275. https://doi.org/10.3390/toxins12040275
30. McKenna A, Hanna M, Banks E, Sivachenko A, Cibulskis K, Kernytsky A, Garimella K, Altshuler D, Gabriel S, Daly M, DePristo MA (2010) The genome analysis toolkit: a MapReduce framework for analyzing next-generation DNA sequencing data. Genome Res 20:1297–1303. https://doi.org/10.1101/gr.107524.110
31. Ramirez-Gonzalez RH, Segovia V, Bird N, Fenwick P, Holdgate S, Berry S, Jack P, Caccamo M, Uauy C (2015) RNA-Seq bulked segregant analysis enables the identification of high-resolution genetic markers for breeding in hexaploid wheat. Plant Biotechnol J 13:613–624. https://doi.org/10.1111/pbi.12281
32. Saile SC, Ackermann FM, Sunil S, Keicher J, Bayless A, Bonardi V, Wan L, Doumane M, Stöbbe E, Jaillais Y, Caillaud MC, Dangl JL, Nishimura MT, Oecking C, El Kasmi F (2021) Arabidopsis ADR1 helper NLR immune receptors localize and function at the plasma membrane in a phospholipid dependent manner. New Phytol 232:2440–2456. https://doi.org/10.1111/nph.17788
33. Shetty NP, Jensen JD, Knudsen A, Finnie C, Geshi N, Blennow A, Collinge DB, Jørgensen HJL (2009) Effects of beta-1,3-glucan from Septoria tritici on structural defence responses in wheat. J Exp Bot 60:4287–4300. https://doi.org/10.1093/jxb/erp269
34. Sissons M, Sissons S, Egan N (2010) Blackpoint status of selected tetraploid species and Australian durum wheats and breeding lines. Crop Sci 50:1279–1286. https://doi.org/10.2135/cropsci2009.08.0439
35. Somma S, Amatulli MT, Masiello M, Moretti A, Logrieco AF (2019) Alternaria species associated to wheat black point identified through a multilocus sequence approach. Int J Food Microbiol 293:34–43. https://doi.org/10.1016/j.ijfoodmicro.2019.01.001
36. Takahashi A, Casais C, Ichimura K, Shirasu K (2003) HSP90 interacts with RAR1 and SGT1 and is essential for RPS2-mediated disease resistance in Arabidopsis. Proc Natl Acad Sci USA 100:11777–11782. https://doi.org/10.1073/pnas.2033934100
37. Tang H, Tan Z, Wang X, Yang L, Chen G, Yu H, Pu Z, Jiang Q, Li M, Cheng M, Qi P, Li W, Liu Y, Wang J (2022) Genome-wide association study of kernel black point resistance in Chinese wheat landraces. Plant Dis 106:1428–1433. https://doi.org/10.1094/pdis-09-21-1898-re
38. The International Wheat Genome Sequencing Consortium, Appels R, Eversole K, Stein N, Feuillet C, Keller B et al (2018) Shifting the limits in wheat research and breeding using a fully annotated reference genome. Science 361:eaar7191. https://doi.org/10.1126/science.aar7191
39. Wang K, Li M, Hakonarson H (2010) ANNOVAR: functional annotation of genetic variants from high-throughput sequencing data. Nucleic Acids Res 38:e164. https://doi.org/10.1093/nar/gkq603
40. Want EJ, Masson P, Michopoulos F, Wilson ID, Theodoridis G, Plumb RS, Shockcor J, Loftus N, Holmes E, Nicholson JK (2013) Global metabolic profiling of animal and human tissues via UPLC-MS. Nat Protoc 8:17–32. https://doi.org/10.1038/nprot.2012.135

41. Wen B, Mei Z, Zeng C, Liu S (2017) metaX: a flexible and comprehensive software for processing metabolomics data. BMC Bioinformatics 18:183. https://doi.org/10.1186/s12859-017-1579-y

42. Xie YR, Raruang Y, Chen ZY, Brown RL, Cleveland TE (2015) *ZmGns*, a maize class I β-1,3-glucanase, is induced by biotic stresses and possesses strong antimicrobial activity. J Integr Plant Biol 57:271–283. https://doi.org/10.1111/jipb.12286

Figures

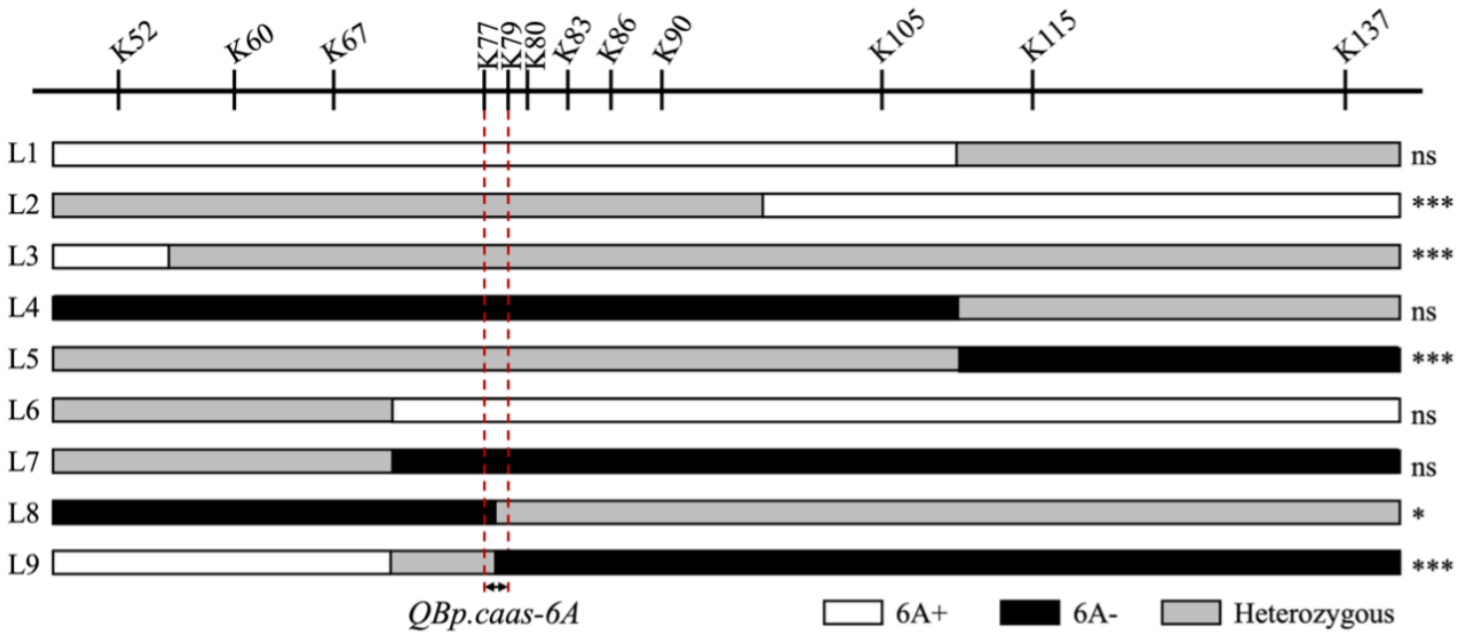

Figure 1

Graphical genotypes (left) and phenotypic assays (right) of nine recombinant types. White, black and gray represent the Zhong 892 (6A+), Linmai 2 (6A−) and heterozygous genotypes, respectively. BP incidence was compared between homozygous 6A+ and 6A− progeny derived from each recombinant. *, ** and *** indicate significance at $P < 0.05$, $P < 0.01$, and $P < 0.001$, respectively; ns, non-significant.

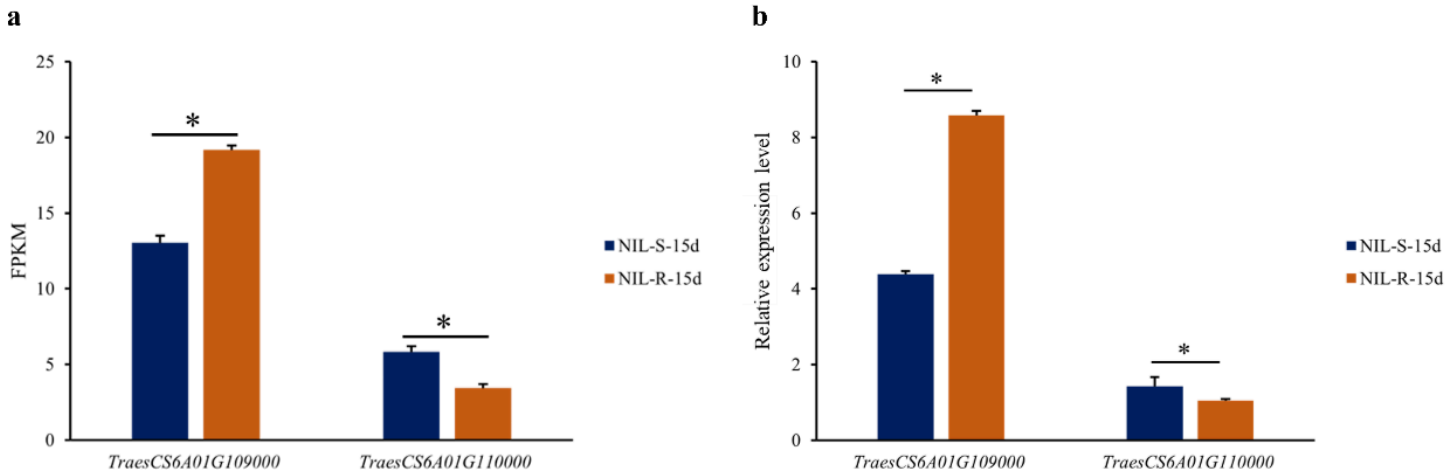

Figure 2

Comparison of gene expression between NIL-S and NIL-R at 15 days after anthesis. **a** Transcriptomic expression, expressed as fragments per kilobase of transcript per million mapped fragments (FPKM), of *TraesCS6A02G109000* and *TraesCS6A02G110000* in the NIL pair. **b** Relative expression of the two genes determined by qRT-PCR. Values are means ± SD from three biological replicates. *, significant at $P < 0.05$.

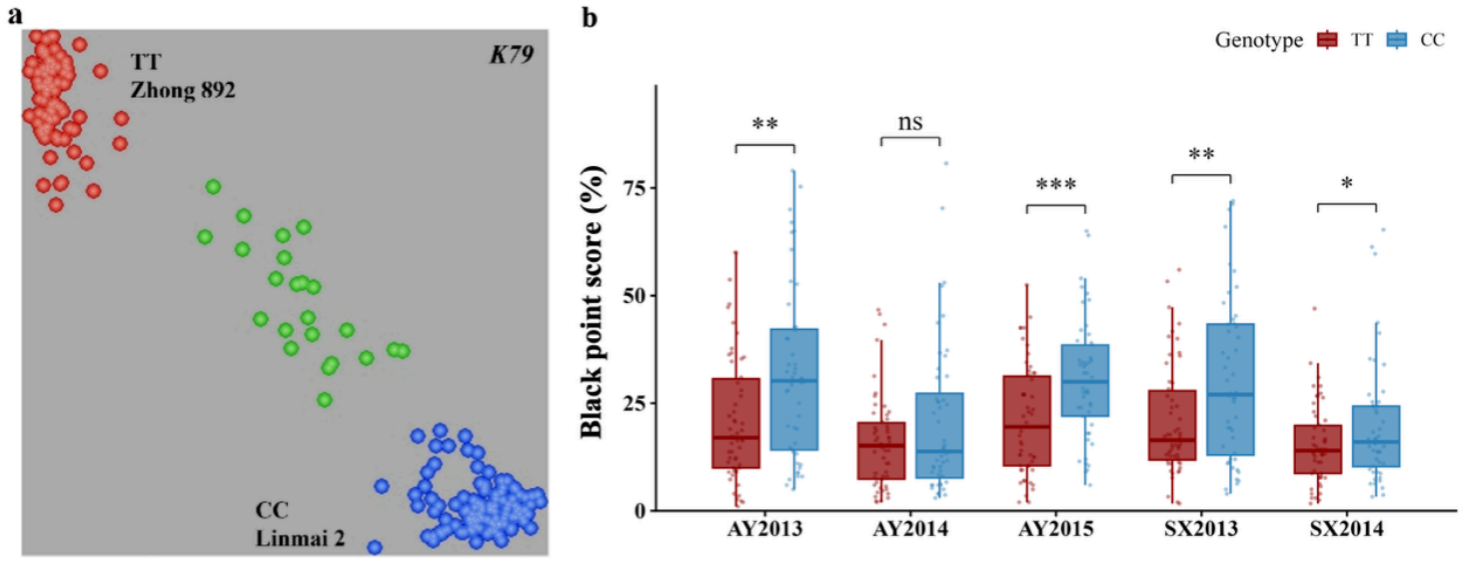

Figure 3

Association of KASP marker *K79* with black point incidence in a panel of 125 wheat cultivars. **a** Distribution of *K79*genotypes in the diversity panel. Red, blue, and green dots represent the Zhong 892 genotype, Linmai 2 genotype, and heterozygotes, respectively. **b**Comparison of black point incidence between cultivars carrying contrasting homozygous genotypes. AY, Anyang; SX, Suixi. *, **, and *** indicate significance at $P < 0.05$, $P < 0.01$, and $P < 0.001$, respectively; ns, not significant.

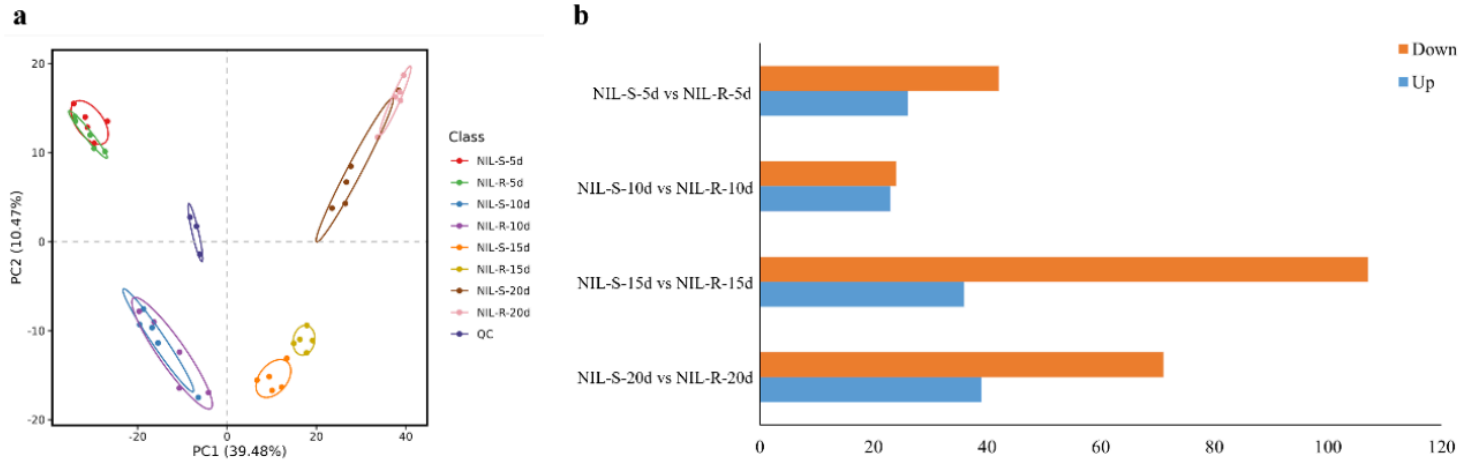

Figure 4

Metabolomic analysis of a pair of near-isogenic lines at 5, 10, 15, and 20 days after anthesis. **a**Principal component analysis score plots for NIL-S and NIL-R at the four developmental stages. Each point represents one of five biological replicates, and ellipses indicate sample groups. **b** Numbers of differentially accumulated metabolites between NIL-S and NIL-R at the four developmental stages.

Supplementary Files

This is a list of supplementary files associated with this preprint. Click to download.

- SuppTables20261104.xlsx
- SuppFigures20261104.docx